ELSEVIER

Journal of Power Sources 70 (1998) 181–199

JOURNAL OF POWER SOURCES

Analytical fuel cell modeling; non-isothermal fuel cells

F. Standaert [a,*], K. Hemmes [b], N. Woudstra [a]

[a] *Delft University of Technology, Department WbMT-EV, PO Box 5037, 2600 GA Delft, The Netherlands*
[b] *Delft University of Technology, Faculty STM, Rotterdamse weg 137, 2628 AL Delft, The Netherlands*

Received 5 December 1996; revised 11 March 1997; accepted 21 April 1997

Abstract

The isothermal fuel cell model, given in an earlier publication, will be generalized to describe the behaviour of non-isothermal fuel cells of co-flow type. To this end the temperature distribution inside a fuel cell in steady state is investigated analytically. A simplified relation between the local temperature and the fuel utilization is derived and its practical significance elucidated. Furthermore, it is shown that the solution of the non-isothermal model is accurately approximated by analytical expressions obtained from a so-called quasi-isothermal approach. This new approach yields a similar expression for the cell voltage as derived from the isothermal model. The quasi-isothermal approach is also used to make a clear comparison between the isothermal and the non-isothermal fuel cell model. © 1998 Elsevier Science S.A.

Keywords: Fuel cells; Analytical model; Cell voltage; Current density distribution; Temperature distribution; Fuel utilization

1. Introduction

In a previous article [1] the setup of an isothermal model for a fuel cell in steady state was given. In this model, the local fuel utilization u and the cell voltage V_{cell} are the solution of an appropriate 'boundary value problem' (BVP), based on the following quasi-ohmic relation for the local current density i

$$V_{eq}(u) - V_{cell} = ri(u) \tag{1}$$

where the local equilibrium potential $V_{eq}(u)$ depends on position through the fuel utilization, u, whereas the quasi-ohmic resistance, r, was assumed to be constant.

An analytical approach for isothermal fuel cells was introduced, based on the linearized Nernst equation

$$V_{eq}^{*}(u) = V_{eq}^{*}(0) - \alpha u \tag{2}$$

The relation between the parameter α in Eq. (2) and the Nernst loss was shown and the accuracy of the analytical results was verified by comparison with numerical computations and measurements on a bench-scale molten carbonate fuel cell (MCFC; 1000 cm^2).

The isothermal model can be applied if the influence of temperature gradients on the local equilibrium potential and the quasi-ohmic resistance is negligible. The local equilibrium potential depends only slightly on temperature [2,3], but the condition of a uniform quasi-ohmic resistance is a major restriction of the isothermal model.

The objective of this article is:

1. to develop a non-isothermal, analytical model for fuel cells with co-flow, and
2. to compare the non-isothermal model with the isothermal model.

The first item will be realized by generalization of the isothermal cell model to a quasi-isothermal model. The setup of the quasi-isothermal model is based on a mathematical method that is similar to 'Duhamel's principle' [4] or the method of

* Corresponding author. Tel.: +31-15-278 52 93; Fax: +31-15-278 24 60.

PII S0378-7753(97)02662-1

'variation of parameters' [5]. The quasi-isothermal model will provide similar expressions for the cell voltage of a non-isothermal fuel cell, as obtained in Ref. [1] for an isothermal fuel cell.

2. Non-isothermal model for fuel cells with co-flow

2.1. Problem definition

As in the isothermal model [1], a rectangular flat plate fuel cell is considered, but the cell temperature and the quasi-ohmic resistance, r, are no longer assumed to be uniform. The other assumptions that underlie the isothermal model will be maintained and are listed in Table 1. The cell part between two cross sections of the cell is called 'subcell'. An example of a subcell is shown in Fig. 1. Since the current collectors will not affect the problem, they are omitted in this figure. Furthermore, it is assumed that the whole cell and all subcells are thermally insulated. During the setup of the model, the generality of this latter assumption with respect to insulated fuel cell stacks will be made clear.

For a fuel cell operating in steady state with co-flow, the temperature will be almost uniform over a cross section of the cell. For instance, temperature differences over a cross section of an MCFC or solid oxide fuel cell (SOFC), with co-flow, are in the order of 10 K [6]. It is, therefore, convenient to assume a uniform gas temperature over a cross section of the cell (assumption 7 in Table 2). Denoting the local temperatures of the anode and cathode gases by T_a and T_c, respectively, this means that

$$T(x) = T_a(x) = T_c(x)$$

Since $T_a(x)$ and $T_c(x)$ are not really identical, the proper $T(x)$ actually represents a mean gas temperature. Nevertheless, the local equilibrium potential depends only slightly on temperature and will be a function of $T(x)$ and, of course, a function of the local gas compositions, in a very good approximation. The quasi-ohmic resistance is usually very sensitive to temperature, but in a first approach it can also be considered as a function of T. Moreover, the expression that will be derived for the local gas temperature, T, requires only a slight modification in order to approximate the hardware temperature. Hence, the small loss in accuracy by considering the quasi-ohmic resistance as a function of T is easy to compensate.

The local fuel utilization in the non-isothermal model will be distinguished from the corresponding variable in the isothermal model, by writing $\tilde{u}$ and u, respectively. As in the isothermal model, the local gas compositions can be calculated from the local fuel utilization $\tilde{u}$. So, neglecting the hydrostatic pressure gradients (assumption 6 in Table 1), the local equilibrium potential $\tilde{V}_{eq}$ and the local quasi-ohmic resistance $\tilde{r}$ can be considered as functions of $\tilde{u}$ and T. Analogously to Eq. (1), the expression for the local overpotential can still be written in accordance with Ohm's law, as

$$\tilde{V}_{eq}[\tilde{u},T] - \tilde{V}_{cell} = \tilde{i}[\tilde{u},T]\tilde{r}[\tilde{u},T] \tag{3}$$

With the use of this current–voltage relation, the BVP derived in Ref. [1] can be generalized to describe also the non-isothermal behaviour of fuel cells.

It is convenient to repeat the original form of this BVP first

$$\left.\begin{aligned} &\frac{du}{dx} = \frac{1}{ri_{in}}\left(V_{eq}[u;T_{cell}] - V_{cell}\right), \quad (0 < x < 1) \\ &u(0) = 0, \quad u(1) = u_1 \end{aligned}\right\} \text{BVP(1) (isothermal)}$$

with x the scaled distance to the cell inlet, u_1 the total fuel utilization, i_{in} the equivalent input current density of the fuel supplied and T_{cell} the uniform cell temperature.

Table 1
Overview of the basic model assumptions, equal to those for the isothermal model [1]

1	Stationary fuel cell (time independent)
2	Large oxidant flow; negligible oxidant utilization with respect to the Nernst loss
3	Changes in fuel composition are significant in the direction of the cell outlet only
4	The local overpotential depends linearly on the local current density through a quasi-ohmic resistance
5	All reactions in the gas phase are in equilibrium
6	Negligible pressure drops (uniform pressure)

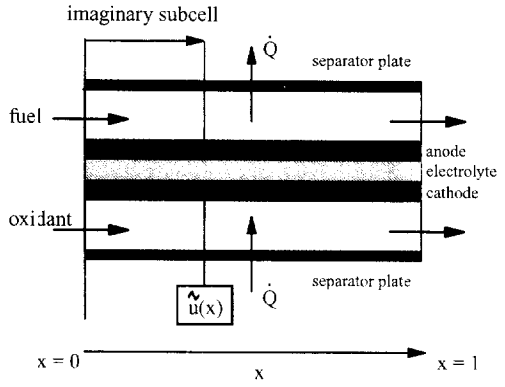

Fig. 1. Longitudinal section of the cell. Without loss of generality the setup of the cell model is restricted to an insulated cell for which the heat transfer $\dot{Q}$ is equal to zero.

Analogously to the derivation of BVP(1), it can be shown from Eq. (3) that the local fuel utilization $\tilde{u}(x)$ and the cell voltage $\tilde{V}_{\text{cell}}$ now satisfy

$$\left.\begin{aligned} &\frac{\mathrm{d}\tilde{u}}{\mathrm{d}x} = \frac{1}{\tilde{r}[\tilde{u},T]i_{in}}\left(\tilde{V}_{\text{eq}}[\tilde{u},T] - \tilde{V}_{\text{cell}}\right), \quad (0 < x < 1) \\ &\tilde{u}(0) = 0, \quad \tilde{u}(1) = u_{\text{f}} \end{aligned}\right\} \text{BVP(2) (non} - \text{isothermal)}$$

In BVP(2) the local temperature and the quasi-ohmic resistance depend on position, whereas in BVP(1) these quantities are uniform. Evidently, for arbitrary quasi-ohmic resistances, r and $\tilde{r}$, the cell voltages in BVP(1) and BVP(2) are not equal. Therefore, the cell voltage in BVP(2) is also marked with a tilde.

When solving BVP(2), we will consider the local temperature as a function of the local fuel utilization $\tilde{u}$, rather than of the position x. It will be shown that the description of T in terms of $\tilde{u}$ is relatively simple and very effective. Once BVP(2) is successively elaborated with an expression for $T(\tilde{u})$ and solved for the set $(\tilde{u}(x),\tilde{V}_{\text{cell}})$, the local current density $\tilde{i}(x)$ can be calculated from the same identity as derived for the isothermal model

$$\tilde{i}(x) = i_{\text{in}}\frac{\mathrm{d}\tilde{u}}{\mathrm{d}x}(x) \quad (0 < x < 1) \tag{4}$$

In a fuel cell stack the operating conditions for the individual cells will vary. Nevertheless, test results suggest that the influence of stacking on the cell performance is limited by applying sophisticated stack designs [7–9]. In that case only the performance of the cells at top and bottom of the stack will be essentially different from the other cells. Consequently, for an insulated stack with co-flow it suffices to consider a single cell, imposing adiabatic boundary conditions [6,10,11]. In fact, if the net heat release through the separator plates of an individual cell would not be zero, heat would be released from all cells (because of their equivalence) and, hence, from the insulated stack as a whole, which is a clear contradiction. Consequently, it is irrelevant whether the separator plates inside the stack are thermally insulating or conducting, since we use a uniform (i.e. mean) temperature over a cross section of the cell. Though the setup of the model is given for an insulated cell, it also holds approximately for one cell of an insulated stack. Since thermal insulation of a whole stack is subject to practical difficulties, many literature data are dedicated to numerical stack models that also simulate the influence of heat transfer from the stack surface to the surroundings ([12–14]). Furthermore, in Ref. [15] the temperature distribution in a fuel cell stack of co-flow type is analytically investigated under the assumptions of a fixed temperature at the stack

Table 2
Extension of the basic model assumptions to the non-isothermal model, and additional assumptions (10 and 11) that underlie the linear relation between temperature and fuel utilization

7	Anode and cathode gases almost have the same local temperature, i.e. the gas temperature, T, is considered to be uniform over a cross section of the cell
8	Thermally insulated cell
9	The cell surface is much larger than a cross section of the cell (practically insulated subcells)
10	Negligible heat production by non-electrochemical reactions in the gas phase
11	The total heat capacity of the process flows is almost uniform (large oxidant flow)

boundary and a uniform heat generation inside the stack. Nevertheless, modeling results show that the major impact of heat release from a stack is restricted to the cells near the stack boundary.

In general, the cell surface is much larger than a cross section of the cell (assumption 9 in Table 2). Because of the relatively small cross section, conduction of heat will hardly contribute to the total transport of heat in the flow direction of the gases [1]. It is realistic to assume that transport of heat in the flow direction happens by means of convection only. Then, all subcells may be considered as being insulated too. It is noted that heat conduction perpendicular to the flow direction is significant, since it has a major contribution to the transfer of heat from the hardware, i.e. the electrode–electrolyte assembly, to the gas flows.

Since all subcells are essentially insulated, the local increase in temperature of the process flows can be calculated from their heat capacities and the local heat production. In Section 2.2 the details of this step will be given and a relation for the local temperature in terms of u will be introduced. In Section 3, a mapping $\tilde{u} \rightarrow u$, that transforms the non-isothermal problem BVP(2) to the isothermal problem BVP(1), will be introduced. The transformed problem will be referred to as the quasi-isothermal problem and can be used to generalize the results and conclusions that are given in Ref. [1] for an isothermal fuel cell.

2.2. Determination of the local temperature

2.2.1. A general expression for the local temperature

Since all subcells are considered to be thermally insulated, energy is transferred across the border of a subcell by the electric current or the gas flows, but not by a heat flux. The entire heat production inside a subcell will contribute to the increase in the temperature of the gas flows. Since the cell is operating in steady state, the temperature of the cell hardware will not change. Only the gases are heated and consequently only the heat capacities of the gas flows will be relevant to determine the temperature rise in the cell. The local heat capacity of the anode flow is denoted by $\dot{m}_a(\tilde{u})c_{p,a}(\tilde{u})$, where $\dot{m}_a(\tilde{u})$ and $c_{p,a}(\tilde{u})$ are, respectively, the local anode mass flow and the corresponding local specific heat at constant pressure. Using a similar notation for the local heat capacity of the cathode flow, the total heat capacity of the anode and cathode flows is given by $\dot{m}_a(\tilde{u})c_{p,a}(\tilde{u}) + \dot{m}_c(\tilde{u})c_{p,c}(\tilde{u})$. This heat capacity is a function of the gas compositions only, assuming that the anode and cathode flows are mixtures of gases with constant specific heats [2]. It determines the amount of heat necessary to achieve an increase in gas temperature, T, of one Kelvin. Hence, the amount of heat related to the temperature rise in an insulated subcell at the cell inlet (see Fig. 1), is given by

$$\left[\dot{m}_a(\tilde{u})c_{p,a}(\tilde{u}) + \dot{m}_c(\tilde{u})c_{p,c}(\tilde{u})\right]\left[T(\tilde{u}) - T(0)\right] \equiv \Delta\dot{H}_{\text{thermal}}\left[\tilde{u}, T - T(0)\right] \tag{5}$$

The quantity $\Delta\dot{H}_{\text{thermal}}$ equals the amount of heat, per unit of time, that would be released if the local gas flows are cooled from the local temperature $T(\tilde{u})$ to the inlet temperature of the cell $T(0)$. Below we will derive an expression for this quantity, from the first law of thermodynamics.

Neglecting changes in potential and kinetic energy of the process flows, the first law states that the heat added to an open system in steady state is equal to the change in enthalpy $\Delta\dot{H}$ of the process flows, per unit time, plus the power, W, that is delivered by the system [17]

$$\dot{Q} = \dot{H}_{\text{out}} - \dot{H}_{\text{in}} + W \equiv \Delta\dot{H} + W \tag{6}$$

The power necessary to achieve changes in the volume of the process flows is taken into account by the term $\Delta\dot{H}$. In the case of a fuel cell, the term W represents the electrical power that is delivered to the external load resistance, i.e. the product of the cell voltage and current. Furthermore, for an insulated subcell the added heat per unit time $\dot{Q}$ is zero. So, for an adiabatic subcell at the cell inlet, in which a fraction $\tilde{u}$ of the fuel supply is utilized, the first law is expressed by

$$W(\tilde{u}) = -\Delta\dot{H}[\tilde{u}, T], \qquad W(\tilde{u}) = \tilde{V}_{\text{cell}} I_{\text{in}} \tilde{u} \tag{7}$$

Changes in thermodynamical state properties, such as the enthalpy, are independent of the many possible ways in which the change of state can be achieved [17]. For example, the change in enthalpy $\Delta\dot{H}[\tilde{u},T]$ could equally well be the result of an isothermal process and a non-isothermal process, successively causing the changes in gas compositions and the increase in temperature. In Fig. 2, these subprocesses are schematized. Without loss of generality we may state that the work, W, is

[1] The justification of this statement follows from a dimension analysis.

[2] The specific heats at constant pressure will be calculated for the average temperature of the fuel cell. Changes in the specific heats due to temperature rise in the cell will be neglected. This is normally allowed, at least for reasonably limited temperature ranges [16].

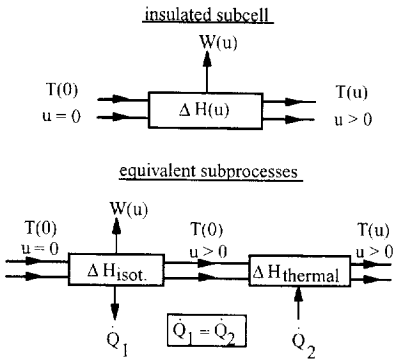

Fig. 2. Schematic representation of the two subprocesses that equal the change in enthalpy of the gas flows through an insulated subcell at the cell inlet.

delivered by the isothermal subprocess only. Then the change in enthalpy in the non-isothermal subprocess is due to heating only. In other words, the second subprocess yields the quantity $\Delta\dot{H}_{\text{thermal}}$ that is needed in Eq. (5)

$$\Delta\dot{H}[\tilde{u},T] = \Delta\dot{H}_{\text{isothermal}}[\tilde{u};T(0)] + \Delta\dot{H}_{\text{thermal}}[\tilde{u},T-T(0)] \tag{8}$$

In Eq. (8), the term $\Delta\dot{H}_{\text{isothermal}}[\tilde{u};T(0)]$ refers to the isothermal enthalpy difference due to changes in the gas compositions. The quantity $-\Delta\dot{H}_{\text{isothermal}}[\tilde{u};T(0)]$ would be the equivalent of the released heat if the gases would be converted in an isothermal system without power generation ($W=0$). However, in a fuel cell the change in enthalphy is controlled by the processes in the electrode–electrolyte assembly and $-\Delta\dot{H}_{isothermal}$ is partially converted into electrical power, see Fig. 2. Unfortunately, it is not fully converted into electrical power and the remaining part still represents a heat production. Since the produced heat cannot be released from the insulated subcell by means of conduction, the temperature of the gases will increase. This gives rise to an extra change in enthalpy, which is represented by the second term on the right-hand side of Eq. (8). The first law (Eq. (7)) relates the net change in enthalpy to the delivered power, W. Substitution of Eq. (8) into Eq. (7) yields

$$\tilde{V}_{\text{cell}} I_{\text{in}} \tilde{u} = -\Delta\dot{H}_{\text{isothermal}}[\tilde{u};T(0)] - \Delta\dot{H}_{\text{thermal}}[\tilde{u},T-T(0)] \tag{9}$$

Using Eq. (9) to elaborate Eq. (5), the local temperature can be written as

$$T(\tilde{u};\tilde{V}_{\text{cell}}) = T(0) + \frac{-\Delta\dot{H}_{\text{isothermal}}[\tilde{u};T(0)] - \tilde{V}_{\text{cell}} I_{\text{in}} \tilde{u}}{\dot{m}_{\text{a}}(\tilde{u}) c_{\text{p,a}}(\tilde{u}) + \dot{m}_{\text{c}}(\tilde{u}) c_{\text{p,c}}(\tilde{u})} \tag{10}$$

Eq. (10) gives the local temperature inside a fuel cell as a function of the local fuel utilization $\tilde{u}$ and the cell voltage, if expressions for $\Delta\dot{H}_{\text{isothermal}}[\tilde{u},T(0)]$ and the total heat capacity of the process flows are available. In the next section simplified expressions for these quantities will be given.

2.2.2. A simplified expression for the local temperature

The obtained expression for the local temperature can be simplified considerably, if heat effects due to chemical reactions in the gas phase are of minor importance (assumption 10 in Table 2). For instance, in general, the heat effect of the water–gas shift reaction is small in comparison with the reaction heat of the overall cell reaction. Hence, the simplified expression for the local temperature will apply to fuel cells without internal reforming.

Usually, a reaction heat at constant pressure is directly proportional to the amount of products converted. However, the reaction heat $\Delta\dot{H}_{\text{isothermal}}[\tilde{u};T(0)]$ was defined with respect to the overall process in the gas phase and is not related to one reaction. Nevertheless, in the case that the heat production by chemical reactions in the gas phase is negligible (assumption

Table 3
Standard gas compositions in mole fractions for an MCFC

Anode inlet gas	H_2	CO	H_2O	CO_2	CH_4
Before equilibrium	0.64	0	0.20	0.16	0
After shift (600°C)	0.57	0.07	0.27	0.09	0
Cathode gas	**Air**	**CO_2**			
Homogeneous	0.70	0.30			

Table 4
Parameter values for an MCFC, corresponding with the standard gas compositions at atmospheric pressure

χ (V)	$c_{p,a}(0)$ (J/kg K)	$c_{p,c}(0)$ (J/kg K)	I_{in} (A)	$\dot{m}_a$ (kg/s)	anode flow volume (cm^3/s)
1.299[a]	2935[b]	1164[b]	1	0.966×10^{-7}	0.59

[a] Value corresponding with an inlet temperature of 600 °C and a total fuel utilization of 95%. Practical values of χ depend slightly on the heat effect of the shift reaction. Without the correction made for the shift reaction, χ would be equal to 1.28 V, irrespective of the total fuel utilization and the gas compositions (see Appendix A).
[b] Values determined with respect to the average cell temperature (650 °C). The values for χ, $c_{p,a}$ and $c_{p,c}$ are based on the JANAF tables.

10 in Table 2), the reaction heat $\Delta\dot{H}_{isothermal}[\tilde{u};T(0)]$ will essentially refer to the overall cell reaction only. Consequently, it will be directly proportional to the fuel utilization $\tilde{u}$, hence to the corresponding output current

$$\Delta\dot{H}_{isothermal}[\tilde{u};T(0)] = -\chi I_{in}\tilde{u} \tag{11}$$

where χ is a constant of proportion (with dimension V). For ideal gases, this constant depends on the inlet temperature, and the overall cell reaction only. In Appendix A, the value of χ is calculated for the reaction of hydrogen with oxygen. However, if also the water–gas shift reaction occurs, assumption 10 is not exactly satisfied and it is convenient to use a slightly modified value for χ (see Table 4 or Appendix A). This modified value depends also on the inlet gas compositions and on the amount of converted CO.

Furthermore, variations in the total heat capacity of the process flows will be small in the case of a large and almost homogeneous oxidant flow. So, it is realistic to treat the total heat capacity as a constant (assumption 11 in Table 2) [3]

$$\dot{m}_a(\tilde{u})c_{p,a}(\tilde{u}) + \dot{m}_c(\tilde{u})c_{p,c}(\tilde{u}) = \dot{m}_a(0)c_{p,a}(0) + \dot{m}_c(0)c_{p,c}(0) \tag{12}$$

Substituting Eqs. (11) and (12) into Eq. (10), we obtain the required expression for the local temperature

$$T(\tilde{u};\tilde{V}_{cell}) = T(0) + \frac{\chi - \tilde{V}_{cell}}{c_{p,a}(0)\dot{m}_a(0) + c_{p,c}(0)\dot{m}_c(0)} I_{in}\tilde{u} \tag{13}$$

Note that this expression for $T(\tilde{u};\tilde{V}_{cell})$ shows a simple, linear dependence on $\tilde{u}$. The term $(\chi - \tilde{V}_{cell})I_{in}\tilde{u}$ in Eq. (13) represents the total heat production inside the fuel cell as a function of the fuel utilization. The term $c_{p,a}(0)\dot{m}_a(0) + c_{p,c}(0)\dot{m}_c(0)$ is the heat capacity of the process flows, based on the inlet gas compositions and the average temperature of the fuel cell (see also the footnotes 2 and 3).

Recall that the set $(\tilde{u}(x),\tilde{V}_{cell})$ has to be calculated from BVP(2), when only the total fuel utilization u_t is imposed as a boundary condition. Next, the total increase in temperature ΔT, defined by

$$\Delta T = T_{outlet} - T_{inlet} = T(u_t;\tilde{V}_{cell}) - T(0)$$

follows from Eq. (13), with $\tilde{u} = u_t$. Another possibility, which will be used in the next section, is to impose both the total fuel utilization and the total increase in temperature ΔT. Then, not only the set $(\tilde{u}(x),\tilde{V}_{cell})$ has to be calculated, but also the amount of oxidant $\dot{m}_c(0)$ required for cooling. Rewriting Eq. (13) for $\tilde{u} = u_t$ and using the definition of ΔT, find

$$\dot{m}_c(0) = \frac{(\chi - \tilde{V}_{cell})I_{out}}{\Delta T \cdot c_{p,c}(0)} - \frac{c_{p,a}(0)}{c_{p,c}(0)}\dot{m}_a(0) > 0 \tag{14}$$

with the total current output I_{out} equal to $I_{in}u_t$. When the oxidant utilization is neglected, the cell voltage $\tilde{V}_{cell}$ is independent of the oxidant supply. In that case, the amount of oxidant required for cooling follows simply from Eq. (14), after the cell voltage has been calculated for the imposed values of ΔT and the cell current I_{out}. When we would take the influence of oxidant utilization on the Nernst loss into account, BVP(2) and Eq. (14) would have to be solved simultaneously.

[3] For an MCFC, the change in the total heat capacity if one mole H_2 reacts with a half mole O_2 is about -7 J/K (650 °C). Based on this value, a more accurate expression for the total heat capacity is given by $\dot{m}_a(0)c_{p,a}(0) + \dot{m}_c(0)c_{p,c}(0) - 7I_{in}\tilde{u}/2F$. The last term in this relation represents the influence of the overall cell reaction on the total heat capacity; the influence of the shift reaction is still neglected. When working with a constant (average) heat capacity, it is recommended to use the value that is obtained by setting $\tilde{u} = 0.5u_t$ in this relation. However, for MCFCs, the difference with the value given by Eq. (12) appears to be relatively small (less than 1% of the total heat capacity) and will be neglected in order to simplify the Eqs. (12)–(14) as much as possible. Nevertheless, in both cases the calculus is the same. Thus adaption of these equations is straightforward.

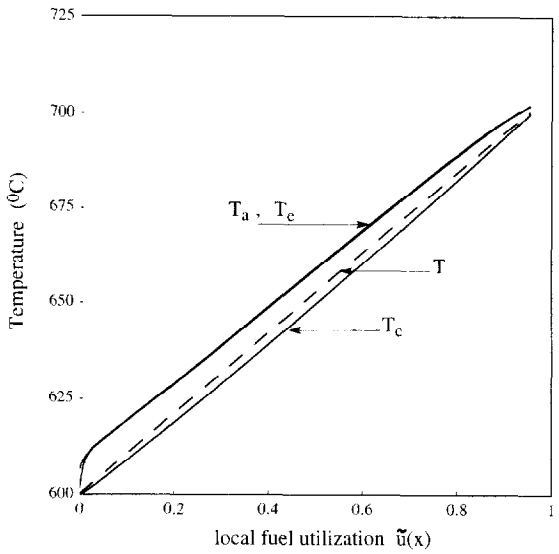

Fig. 3. Numerical results for the local temperatures inside an MCFC with co-flow, obtained from a detailed numerical model [6] (T_a: anode flow, T_c: cathode flow, T_e: electrode–electrolyte assembly). For comparison also the temperature, T, as calculated from the linear relation in Eq. (13), is shown.

An analytical expression for the cell voltage will be derived later. First, the accuracy of the simplified expression in Eq. (14) will be verified, using a detailed numerical cell model by De Groot [6]. As an example, we consider an MCFC with standard gas supply (see Table 3) at an inlet temperature of 600 °C. The corresponding values for χ, $c_{p,a}$ and $c_{p,c}$ are given in Table 4. In this Table also the amount of fuel that corresponds with an equivalent input current of 1 A is given. From this latter value the necessary amount of fuel can easily be calculated if the cell surface, the average current density and the total fuel utilization are known: for a 1000 cm^2 MCFC, with a current density of 157 mA/cm^2 (I_{out} = 157 A) and a total fuel utilization of 95% ($u_1 = 0.95$), the anode mass supply is given by $\dot{m}_a(0) = (157/0.95) \times 0.966 \times 10^{-7} = 1.60 \times 10^{-5}$ kg/s. Furthermore, ΔT will be set equal to 100 K.

Extensive numerical computations that take into account variations in temperature over a cross section of the cell as well as the utilization of oxidant, the heat release of the shift reaction and changes in the specific heats at constant pressure [4], yield a cell voltage of 0.75 V. The numerically calculated value for the oxidant mass flow is 7.02×10^{-4} kg/s, compared with 7.00×10^{-4} kg/s that follows from Eq. (14). For this example the relative error in the analytical expression for $\dot{m}_c(0)$ is only 0.3%. In spite of all the assumptions made, the oxidant mass flow is accurately calculated from Eq. (14), under the condition that the cell voltage is accurately known [5]. In the previous example, a very high value for the total fuel utilization u_1 was imposed ($u_1 = 0.95$). In principle, the validity of Eq. (14) is not restricted to moderate values of u_1, but the analytical expression for the cell voltage being introduced in the next section will not allow for very high values of u_1.

In Fig. 3, the numerically calculated temperature distribution is plotted as a function of the local fuel utilization $\tilde{u}(x)$, for the anode gases as well as for the cathode gases. Clearly, both temperatures T_a and T_c depend linearly on the fuel utilization in very good approximation. Solids and liquids are good heat conductors in comparison with gases. Consequently, the electrodes and the electrolyte are practically at the same temperature, say T_e, at any cross section. As indicated in the figure, the local temperature of the anode flow almost coincides with the hardware temperature T_e. It can be shown that this is due to the fact that only a small amount of heat has to be transferred to the relatively small anode flow. The large cathode flow is used for cooling and so a serious temperature difference between the hardware and cathode gas will exist. Since the anode gas temperature T_a represents the local temperature of the electrode–electrolyte assembly very well, it should be used to determine the quasi-ohmic resistance. However, the introduced mean gas temperature T is the temperature of the gas mixture that would be obtained by mixing of the local anode and cathode flows. As illustrated by the figure, T is mainly determined by the temperature of the large cathode flow.

[4] In the numerical model [6] the specific heats $c_{p,a}$ and $c_{p,c}$ are considered as functions of both temperature and gas compositions.

[5] Moreover, not all simplifications are essential in order to obtain an expression for $\dot{m}_c(0)$. For instance, instead of Eq. (12), a more accurate average value for the total heat capacity can be used (see Footnote 3). For the MCFC example, the relative error in $\dot{m}_c(0)$ then reduces from 0.3 to 0.1%. Furthermore, in order to eliminate assumption 7 in Table 2, the last term in Eq. (14) can be replaced by $[c_{p,a}(0)(T_{a,outlet} - T_{inlet})/c_{p,c}(0)(T_{c,outlet} - T_{inlet})]\dot{m}_a(0)$. Then, still one inlet temperature is assumed for both process flows and ΔT is defined as $T_{c,outlet} - T_{inlet}$.

3. Quasi-isothermal approach for an MCFC with co-flow

3.1. Problem definition for an MCFC, based on a linearized Nernst equation and a simple expression for $\tilde{r}$

Now that we have expressed the local temperature in terms of the fuel utilization, BVP(2) can be reduced to a model problem equivalent with the isothermal 'analytical cell model' introduced in Ref. [1]. To avoid extended mathematics, this so-called quasi-isothermal approach will be demonstrated by a simple MCFC example, though the method itself is quite general.

We consider an MCFC with co-flow and standard gas supply (see Table 3). Of all parameters influencing the quasi-ohmic resistance (i.e. the polarization losses), the local temperature is the most important. For reasons of simplicity we assume that the quasi-ohmic resistance is a function of the temperature only. Furthermore, the temperature of the gas flows increases from 600 °C at the cell inlet ($\tilde{u} = 0$) to 700 °C at the outlet ($\tilde{u} = u_1$). Hence, the linear relation for the local temperature, based on the assumptions 10 and 11 in Table 2, reads

$$T(\tilde{u}) = T_{\text{inlet}} + \Delta T\frac{\tilde{u}}{u_1} = 873 + 100\frac{\tilde{u}}{u_1} \quad (0 \le \tilde{u} \le u_1) \tag{15}$$

Recall that the corresponding amount of coolant can easily be calculated once the cell voltage is known. The purpose of this section is to obtain expressions for both the cell voltage and the local current density.

The temperature dependence of the quasi-ohmic resistance $\tilde{r}$ is often described by one or more Arrhenius terms [10,12]. Here, we will focus on a single Arrhenius term, i.e. we consider the following simplified expression for the quasi-ohmic resistance

$$\tilde{r}(T) = \tilde{r}(873)\exp\left[A\left(\frac{1}{T} - \frac{1}{873}\right)\right] \tag{16}$$

where A is a constant. This relation is convenient for a simple analysis and simulates actual quasi-ohmic resistances quite well, at least for the relevant temperature range and a suitable value for A. A convenient expression for the reciprocal value of T, in terms of $\tilde{u}$, is obtained by expanding Eq. (15)

$$\frac{1}{T(\tilde{u})} = \frac{1}{873\left(1 + \frac{100}{873}\frac{\tilde{u}}{u_1}\right)} \approx \frac{1}{873}\left(1 - \frac{100}{873}\frac{\tilde{u}}{u_1} + 0.007\right) \quad (0 \le \tilde{u} \le u_1) \tag{17}$$

where the relative error is less than 1%. Substitution of Eq. (17) into Eq. (16), yields

$$\tilde{r}(\tilde{u}) = \tilde{r}(0)\exp\left(-\lambda\frac{\tilde{u}}{u_1}\right) \quad (0 \le \tilde{u} \le u_1) \tag{18}$$

where λ is a constant, related to A. However, λ is fully determined if $\tilde{r}(0)$ as well as the value of $\tilde{r}$ at the cell outlet, i.e. $\tilde{r}(u_1)$, are imposed

$$\lambda = -\ln\frac{\tilde{r}(u_1)}{\tilde{r}(0)} \quad (\lambda \ge 0;\ \lambda = 0 \text{ for an isothermal cell}) \tag{19}$$

In the case of standard gas compositions, typical values are $\tilde{r}(0) = 1.46\ \Omega\ \text{cm}^2$ (600 °C) and $\tilde{r}(u_1) = 0.8\ \Omega\ \text{cm}^2$ (700°C). Thus, from Eq. (19), it follows that λ is typically 0.6.

Although the equilibrium constant, K, for the reverse shift reaction is a function of the local temperature, the local equilibrium potential is reasonably well determined by using an average value for K, throughout the cell (i.e. $K = 0.5$ at 650 °C). Then the expression for the local equilibrium potential in terms of $\tilde{u}$ and T is the same as for the isothermal model (see Appendix A in Ref. [1]). But now the local temperature, T, depends on the local fuel utilization $\tilde{u}$ through the linear relation in Eq. (15)

$$\tilde{V}_{\text{eq}}[\tilde{u},T] = E(T) - \frac{RT}{2F}f(\tilde{u};K) \tag{20}$$

The explicit expression for the function $f(\tilde{u}, K)$ is rather complicated and is not presented here (see Ref. [1]). The reference potential $E(T)$ in Eq. (20) would be the open-circuit voltage (OCV) of the cell, if T would be the inlet temperature. The value of E is determined by thermodynamics and appears to be a linear function of temperature in very good approximation [3]. Therefore, a constant value for the partial derivative of E with respect to T will be used.

In the isothermal model the parameter, α, was introduced to describe the utilization polarization (or Nernst loss). It represents a characteristic value for the decrease in the local equilibrium potential due to fuel utilization and is defined as the partial derivative of $-V_{eq}[u,T]$ with respect to u; the derivative at constant temperature. Analogous, the parameter $\tilde{\alpha}$ in the non-isothermal model will represent a characteristic value for the total derivative of $-\tilde{V}_{eq}[\tilde{u},T(\tilde{u})]$ with respect to $\tilde{u}$. Based on Eq. (15), a characteristic value for this total derivative derives from considerations made in Appendix A [6]

$$\tilde{\alpha} = \alpha + \frac{100}{u_1}\left(\frac{0.5}{923}\alpha - \frac{\partial E}{\partial T}\right) = \text{constant} \tag{21}$$

Hence, as E is a slightly decreasing function of temperature, the parameter $\tilde{\alpha}$ in the non-isothermal model will be somewhat larger than the α in the isothermal model. Analogously to Eq. (2), the linearized version $\tilde{V}_{eq}^{*}$ of the local equilibrium potential $\tilde{V}_{eq}$ in the non-isothermal model is given by

$$\tilde{V}_{eq}^{*}[\tilde{u},T(\tilde{u})] = \tilde{V}_{eq}^{*}[0,T(0)] - \tilde{\alpha}\tilde{u} \tag{22}$$

Now that we have expressed the local equilibrium potential and the quasi-ohmic resistance in terms of the local fuel utilization $\tilde{u}$ only, the BVP(2) can be solved for $\tilde{u}$ and $\tilde{V}_{cell}$. To this end, either the non-linearized Nernst Eq. (20) or the linear approximation in Eq. (22) can be used. It is emphasized that numerical results will be based on the non-linearized Nernst equation, whereas analytical results will be based on the linearized Nernst equation. The cases $\tilde{\alpha} = 0$ and $\tilde{\alpha} > 0$ will be treated separately. The case $\tilde{\alpha} = 0$ is hypothetical and easy to solve. Its solution will be used as a reference solution to show clearly the effect of gas utilization, in practical cases where $\tilde{\alpha} > 0$.

3.2. Solution for $\tilde{\alpha} = 0$

In the hypothetical case that the local equilibrium potential is independent of gas utilization, i.e. $\tilde{\alpha} = 0$, solving BVP(2) is straightforward. The solution is then given by

$$\tilde{u}(x) = -\frac{u_1}{\lambda}\ln(1-\gamma\lambda x), \qquad \tilde{V}_{cell} = V_{eq}[0,T(0)] - \langle\tilde{r}\rangle i_{in}u_1 \tag{23}$$

where $\langle\tilde{r}\rangle$ is the average value of the quasi-ohmic resistance and γ is a constant. Respectively, they are defined by

$$\langle\tilde{r}\rangle = \frac{1}{u_1}\int_0^{u_1}\tilde{r}(\tilde{u})\,\mathrm{d}\tilde{u} = \frac{\tilde{r}(0)-\tilde{r}(u_1)}{\ln[\tilde{r}(0)]-\ln[\tilde{r}(u_1)]} \tag{24}$$

$$\gamma = \frac{\langle\tilde{r}\rangle}{\tilde{r}(0)} = \frac{1-\exp(-\lambda)}{\lambda}, \quad (0<\gamma\le 1;\ \gamma = 1 \text{ for } \lambda = 0) \tag{25}$$

For an isothermal fuel cell ($\lambda = 0$) the constant γ is determined by the limiting value of Eq. (25) for $\lambda \to 0$.

An expression for the local current density easily follows from the solution given by Eq. (23)

$$\tilde{i}(x) = i_{in}\frac{\mathrm{d}\tilde{u}}{\mathrm{d}x}(x) = \frac{\gamma i_{out}}{1-\gamma\lambda x} \tag{26}$$

with i_{out} the average current density, being equal to $i_{in}u_1$. Since $\gamma\lambda$ is a constant smaller than unity, the local current density $i(x)$ is monotonously increasing, in agreement with the assumptions of a uniform equilibrium potential and a monotonously decreasing quasi-ohmic resistance. This behaviour of the local current density changes drastically for realistic values of $\tilde{\alpha} \neq 0$.

3.3. Solution for $\tilde{\alpha} > 0$

In general, BVP(2) is rather complicated since the local equilibrium potential will be a decreasing function of the fuel utilization. However, without a significant loss in accuracy the non-isothermal model can be simplified to an analytical model that is equivalent to BVP(1) for the isothermal model [1].

[6] In fact, K is about 0.4 at 600 °C and about 0.67 at 700 °C. The inaccuracy in Eq. (21), introduced by taking $K = 0.5$, can be expressed by a correction term (see Appendix A). For the standard fuel composition, it follows that the $\tilde{\alpha}$ obtained from Eq. (21) deviates considerably less than 6 mV from the $\tilde{\alpha}$ based on the actual $K(t)$. The effect of this inaccuracy on the final value for the cell voltage will be less than 3 mV (a relative error of less than 0.5%). The local equilibrium potential will become more sensitive for the precise value of $K(T)$ if the partial pressure of CO increases. Hence, if the fuel is rich in CO, the result of Eq. (21) may be inaccurate.

The quasi-isothermal problem formulation is based on the mapping $\tilde{u} \rightarrow u$, given by the solution of the following initial value problem

$$\frac{\mathrm{d}u}{\mathrm{d}\tilde{u}} = \frac{\tilde{r}(\tilde{u})}{\langle \tilde{r} \rangle} \quad (0 < \tilde{u} < u_1) \quad u(0) = 0 \tag{27}$$

The end value for u is obtained by integration of Eq. (27) from $\tilde{u} = 0$ to $\tilde{u} = u_1$. In this way (see also Eq. (24)) it follows that the end values for u and $\tilde{u}$ are equal. Hence, the mapping $\tilde{u} \rightarrow u$ does not change the boundary conditions

$$u(0) = \tilde{u}(0) = 0 \qquad u(1) = \tilde{u}(1) = u_1 \tag{28}$$

The derivative of u with respect to x is obtained from Eq. (27) by applying the chain rule

$$\frac{\mathrm{d}u}{\mathrm{d}x} = \frac{\mathrm{d}u}{\mathrm{d}\tilde{u}} \frac{\mathrm{d}\tilde{u}}{\mathrm{d}x} = \frac{\tilde{r}(\tilde{u})}{\langle \tilde{r} \rangle} \frac{\mathrm{d}\tilde{u}}{\mathrm{d}x} \tag{29}$$

Eq. (29) can be used to eliminate the variable quasi-ohmic resistance and the meantime derivative $\mathrm{d}\tilde{u}/\mathrm{d}x$ from the ODE for $\tilde{u}$ in BVP(2). In this way the ODE for $\tilde{u}$ transforms into an ODE for u

$$\frac{\mathrm{d}u}{\mathrm{d}x} = \frac{1}{\langle \tilde{r} \rangle i_{\mathrm{in}}} \left(\tilde{V}^*_{\mathrm{eq}}[0,T(0)] - \tilde{\alpha}\,\tilde{u}(u) - \tilde{V}^*_{\mathrm{cell}} \right) \tag{30}$$

where $\tilde{V}_{\mathrm{cell}}$ is replaced by $\tilde{V}^*_{\mathrm{cell}}$ to indicate that the cell voltage is based on the linearized Nernst equation. By using the linearized Nernst equation, the obtained ODE can be solved analytically in very good approximation, after which a solution for $\tilde{u}$ is obtained by application of the inverse mapping $u \rightarrow \tilde{u}$. For the quasi-ohmic resistance defined by Eq. (18), the solution $u(\tilde{u})$ of Eq. (27) and the corresponding inverse mapping are given by, respectively

$$u(\tilde{u}) = \frac{u_1}{\gamma\lambda}\left[1 - \exp\left(-\lambda\frac{\tilde{u}}{u_1}\right)\right] \qquad \tilde{u}(u) = -\frac{u_1}{\lambda}\ln\left(1 - \gamma\lambda\frac{u}{u_1}\right) \tag{31}$$

Using the second part of Eq. (31), the local equilibrium potential in Eq. (30) can be expressed in terms of u

$$\tilde{V}^*_{\mathrm{eq}}[0,T(0)] - \tilde{\alpha}\,\tilde{u} = \tilde{V}^*_{\mathrm{eq}}[0,T(0)] + \tilde{\alpha}\frac{u_1}{\lambda}\ln\left(1 - \gamma\lambda\frac{u}{u_1}\right) \tag{32}$$

The functions $u(x)$ and $\tilde{u}(x)$ are equal at the boundaries (Eq. (28)) and will be slightly different for intermediate values of x. Nevertheless, consider also the following linear approximation of Eq. (32), obtained by setting $\tilde{u}(x) = u(x)$ for all x

$$\tilde{V}^*_{\mathrm{eq}}[0,T(0)] - \tilde{\alpha}\,\tilde{u} \approx \tilde{V}^*_{\mathrm{eq}}[0,T(0)] - \tilde{\alpha}\,u \tag{33}$$

For practical values of $\lambda > 0$, this approximation for the local equilibrium potential, as a function of the transformed variable u, will be somewhat too small, but nevertheless reasonably accurate. For instance, for $\lambda = 0.6$, $\tilde{\alpha} \approx 0.2$ V and $u_1 = 0.8$, the maximum deviation in the approximation is easily calculated to be about -10 mV, which is small in comparison with the value of $\tilde{\alpha}$.

In Appendix A it is shown that substitution of Eq. (33) into Eq. (30) is allowed, if in the latter equation the average value $\langle \tilde{r} \rangle$ is replaced by a somewhat lower value in order to compensate for this artificial decrease of the local equilibrium potential. The replacement of $\langle \tilde{r} \rangle$ will be denoted by r_{m}. In this way, a problem formulation for a non-isothermal fuel cell is obtained that is much the same as BVP(1) for the isothermal model. Therefore, this so-called quasi-isothermal problem formulation will be referred to as BVP(1′).

3.3.1. *Quasi-isothermal problem formulation*

$$\left.\begin{aligned} &\frac{\mathrm{d}u}{\mathrm{d}x} = \frac{1}{r_{\mathrm{m}} i_{\mathrm{in}}}\left(\tilde{V}^*_{\mathrm{eq}}[0,T(0)] - \tilde{\alpha}\,u - \tilde{V}^*_{\mathrm{cell}}\right) \quad (0 < x < 1) \\ &u(0) = 0 \qquad u(1) = u_1 \end{aligned}\right\} \text{BVP(1′)}$$

As shown in Appendix A, the mean value r_{m} for the quasi-ohmic resistance is accurately approximated by

$$r_{\mathrm{m}} = \langle \tilde{r} \rangle \cdot (1 - \delta), \text{with } \delta \approx \begin{cases} 0 & \text{for } \lambda = 0 \\ \dfrac{\tilde{\alpha}}{\tilde{\alpha} + 2\langle \tilde{r} \rangle i_{\mathrm{in}}}\left(\dfrac{2}{\gamma\lambda} - \dfrac{2}{\lambda} - 1\right) > 0 & \text{for } \lambda > 0 \end{cases} \tag{34}$$

The analytical expression for the small correction term δ is fairly accurate if the artificial decrease in the local equilibrium potential (the difference between the Eqs. (32) and (33)) is small, i.e. for moderate values of λ. Recall that $\lambda = 0$ if the quasi-ohmic resistance is independent of position, i.e. for the isothermal model. Apparently, δ is due to the non-uniformity of $\tilde{r}$. In Appendix B it is shown that a homogeneous distribution of the quasi-ohmic losses is favourable with respect to the cell voltage. It is straightforward to verify that the variable resistance $\tilde{r}$ (decreasing from cell inlet to cell outlet) will cause a more homogeneous distribution of the quasi-ohmic losses than a uniform average resistance $\langle \tilde{r} \rangle$ [7]. In Eq. (34), the advantage of the variable quasi-ohmic resistance is expressed by the term $(1 - \delta)$.

Note also that the so-called quasi-isothermal approach is, in fact, a special case of the isothermal problem formulation by BVP(1) in Section 2.1. That is, the quasi-isothermal problem BVP(1') is obtained by using the following parameter settings in BVP(1), with linearized Nernst Eq. (2)

$$r \to r_m, \quad \alpha \to \tilde{\alpha}, \quad V_{eq}^*(0) \to \tilde{V}_{eq}^*[0,T(0)]$$

Once BVP(1') is solved for the set $(u(x),\tilde{V}_{cell}^*)$, the actual $\tilde{u}(x)$ is obtained from the inverse mapping $\tilde{u}(u)$ given by Eq. (31).

3.3.2. Solution

Mathematically BVP(1') is the same as the isothermal 'analytical cell model', presented in Ref. [1]. Only the parameters have a slightly different value, which is indicated by the tilde '~'. The solution of the isothermal 'analytical cell model' given in Ref. [1], directly applies to BVP(1') by using the parameter settings given above.

For instance, a convenient and accurate expression for the cell voltage is obtained from Eq. (18) in [1]

$$\tilde{V}_{cell}^* \approx \tilde{V}_{eq}^*[0,T(0)] - \frac{1}{2}\tilde{\alpha}u_1 - r_m i_{out} - \frac{1}{3}\tilde{Z}^2 r_m i_{out} \quad \text{(first order approximation)} \tag{35}$$

where the number $\tilde{Z}$ is defined by

$$\tilde{Z} = \frac{\tilde{\alpha}}{2 r_m i_{in}}$$

Analogous to the derivation given in the isothermal model, it can be shown that the term $\tilde{\alpha}u_1/2$ in Eq. (35) represents the Nernst loss. The last two terms in Eq (35) are voltage losses due to the quasi-ohmic resistance $\tilde{r}$.

Next, consider the following expression for u, obtained from Eq. (10) in Ref. [1]:

$$u(x;i_{in}) = \frac{\tilde{V}_{eq}^*(0) - V_{cell}^*}{\tilde{\alpha}}\left[1 - \exp\left(\frac{-\tilde{\alpha}x}{r_m i_{in}}\right)\right] \tag{36}$$

The corresponding current distribution in the isothermal model follows from the identity $i(x) = i_{in}\, du/dx$

$$i(x;i_{in}) = \frac{\tilde{V}_{eq}^*[0,T(0)] - \tilde{V}_{cell}^*}{r_m}\exp\left(-\frac{\tilde{\alpha}}{r_m i_{in}}x\right) \tag{37}$$

An expression for the local current density $\tilde{i}(x)$ in the non-isothermal model follows from Eq. (36), by using the mapping $\tilde{u}(u)$ (Eq. (31) with $\gamma = r_m/\tilde{r}(0)$) and the identity $\tilde{i}(x) = i_{in}d\tilde{u}/dx = i(x)d\tilde{u}/du$

$$\tilde{i}(x;i_{in}) \approx i(x;i_{in})/\left[\frac{\tilde{r}(0)}{r_m} - \lambda\frac{u(x;i_{in})}{u_1}\right] \tag{38}$$

Eqs. (35) and (38) for the cell voltage and the local current density are accurate as long as the linearization of the Nernst equation is accurate, i.e. up to a fuel utilization of about 80%. The following examples will illustrate this.

Fig. 4 shows the cell voltage of the non-isothermal MCFC, as a function of the total fuel utilization u_1, according to several approximations. All the results correspond with an average output current density i_{out} equal to 150 mA/cm^2. Curve A is obtained from the analytical expression in Eq. (35). Numerical computations (curve B) clearly show the accuracy of the analytical results for $u_1 \leq 0.8$. At the current state-of-the-art, practical values for u_1 usually lie between 0.75 and 0.9. Even up to an utilization of 90%, the analytical results show reasonably good agreement with the numerical computations. However, in practice, the cell voltage may deviate earlier (i.e. for smaller values of u_1) and faster from the analytical

[7] In both cases, the local overpotential decreases from inlet to outlet. The local quasi-ohmic losses $\tilde{r}\tilde{i}^2$ are directly related to the (square of the) local overpotential and the quasi-ohmic resistance from Eq. (3).

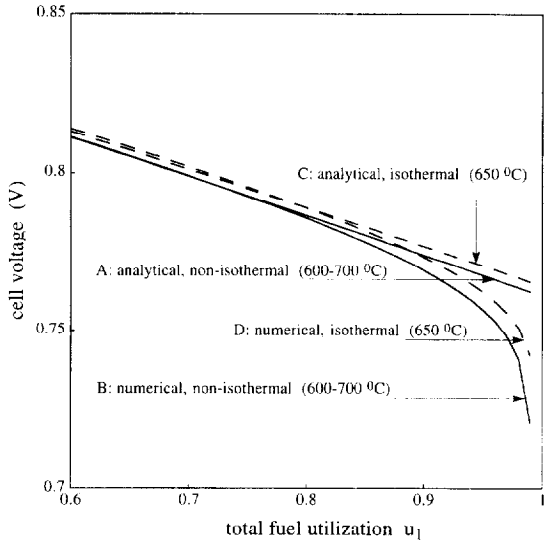

Fig. 4. Cell voltage of an MCFC as a function of the total fuel utilization u_1 for a constant average current density of 150 mA/cm^2. Curve A: from Eq. (35); curve B: from numerical computations, based on BVP(2) with non-linearized Nernst equation; curves C and D: from the isothermal model [1]. (Standard gas supply (Table 3), oxidant utilization is neglected, for parameter values see Table 5.)

solution than the numerical results suggest. Because, at high fuel utilizations, the partial pressure of hydrogen is very low and an additional concentration polarization may occur as a result of slow mass transport rates in or near the electrodes. Evidently, the impact of this effect also depends on the average current density i_{out}. However, since we assumed $\tilde{r}$ to be an explicit function of temperature only, the additional concentration polarization is not incorporated in our model explicitly. Anyway, for (very) high values of u_1 or i_{out}, the imposed values for $\tilde{r}(0)$ and $\tilde{r}(u_1)$, or even the entire expression for $\tilde{r}(\tilde{u})$, has to be corrected in order to obtain a more realistic picture. But this step is beyond the scope of this article and will be omitted.

In Fig. 4, also the cell voltage according to the isothermal parameters, instead of the quasi-isothermal parameters, is plotted (curves C and D). The parameter values for the several curves are given in Table 5. The analytical value $\tilde{\alpha} = 0.22$ V presented in this Table corresponds with a total fuel utilization of 80% and a negligible oxidant utilization. In practice, oxidant utilization will have a small influence and consequently the actual value of $\tilde{\alpha}$ will be somewhat higher (numerical calculations that take into account the utilization of oxidant yield an $\tilde{\alpha}$ of about 0.24 V). The parameter C that appears in Table 5 will be explained in Section 3.4.

Fig. 5 shows the current distribution inside the non-isothermal MCFC for a total fuel utilization of 80% and an average current density of 150 mA/cm^2. Curve A_1 is obtained from the analytical approximation in Eq. (38) and shows reasonably good agreement with numerical computations (curve B). The deviations are mainly due to the linearization of Eq. (32), which was the origin of the artificial loss in the equilibrium potential. Consequently, the analytical approximation yields an average current density that is sometimes too small. Curve A_2 is obtained from a very accurate analytical expression, which will be introduced next.

Table 5
Parameter values accompanying Figs. 4 and 5 (standard gas supply, $T(0) = 600$°C)

Curve	OCV (V)	α (V)	$\tilde{\alpha}$ (V)	r (Ω cm^2)	r_m (Ω cm^2)	$\partial E/\partial T$ (V/K)	C (V)
A	$\tilde{V}_{eq}^*[0,T(0)] = 1.045$ [a]	0.18	0.22 [b]		1.05 [d]	-0.02×10^{-2}	0.003
B	$\tilde{V}_{eq}[0,T(0)] = 1.07$					-0.02×10^{-2}	
C	$V_{eq}^*[0;923] = 1.03$	0.18		1.08 [c]			0.003
D	$V_{eq}[0;923] = 1.06$			1.08 [c]			

[a] For $u_1 = 0.8$. Determined from Eq. (22) and the condition $\tilde{V}_{eq}^*[u_1/2,T(u_1/2)] = V_{eq}^*[u_1/2;923]$, using $V_{eq}^*[u_1/2;923] = 0.958$ V as a result from Eq. (2).

[b] Obtained from Eq. (21) for $u_1 = 0.8$.

[c] The quasi-ohmic resistance at 650 °C is given by $r \equiv \tilde{r}(u_1/2) = 1.08$ (Ω cm^2), from Eq. (18).

[d] Value derived from Eq. (34), using $\lambda = 0.6$ and $\gamma = 0.75$ (Eq. (25)), corresponding with $\tilde{r}(0) = 1.46$ and $\tilde{r}(u_1) = 0.8$ (Ω cm^2).

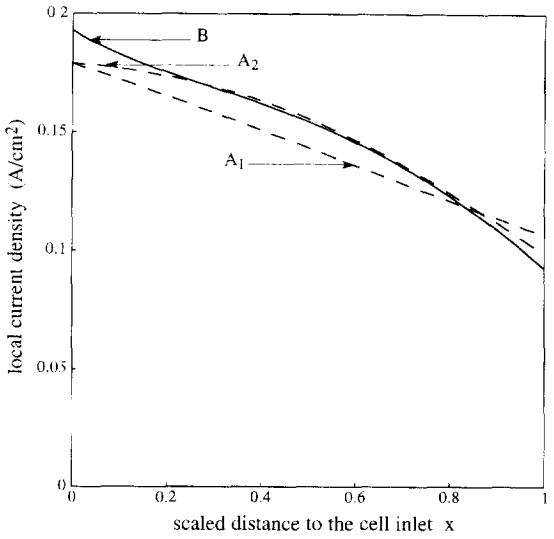

Fig. 5. Current distribution in a non-isothermal MCFC, according to several approximations. Curve A_1: from Eq. (38); curve A_2: from Eq. (40); curve B shows the results of numerical computations, based on BVP(2) with non-linearized Nernst equation. The average current density is 150 mA/cm^2 at a total fuel utilization of 80%. (Standard gas supply (Table 3), $T(0) = 600$ °C, $\Delta T = 100$ K, oxidant utilization is neglected, for parameter values see Table 5 (A and B)).

3.4. Extended relations for the cell voltage and the local current density

Inaccuracies in the analytical expression for the cell voltage (Eq. (35)) occur as a consequence of the so-called initial dip in the non-linearized Nernst equation. This initial dip is the deviation of the equilibrium potential from its linear approximation for small fuel utilizations and was neglected in the analytical approach. The obtained expression for the local current density (Eq. (38)) is somewhat less accurate than the expression for the cell voltage, since it is also based on the linearization of Eq. (33). First, the inaccuracies due to this extra linearization will be diminished. Next, a slightly modified expression for the cell voltage will be introduced, that accounts for the influence of the initial dip in the Nernst equation.

It is convenient (see Appendix A) to introduce a quantity, i_{in}^{ext}, which deviates slightly from the equivalent input current density i_{in}

$$i_{in}^{ext} = \frac{\tilde{Z}}{\tilde{Z} + \delta} i_{in} \tag{39}$$

The extended relation for the local current density is referred to as $\tilde{i}_{ext}$ and is given by

$$\tilde{i}_{ext}(x; i_{in}) \approx \tilde{i}(x; i_{in}^{ext}) \frac{1}{1 - Y(x; i_{in}^{ext})} \tag{40}$$

where $\tilde{i}$ is defined by Eq. (38) and $Y(x; i_{in}^{ext})$ is defined by

$$Y(x; i_{in}^{ext}) = \frac{2\tilde{Z}}{\left[u_1 - 2u(x, i_{in}^{ext})\right]\tilde{Z} + u_1} \left[u(x, i_{in}^{ext}) + \frac{u_1}{\lambda} \ln\left(1 - \gamma\lambda \frac{u(x, i_{in}^{ext})}{u_1}\right)\right]$$

Note that $\tilde{\alpha}$ times the last factor in the expression for $Y(x)$ is equal to the artificial loss in equilibrium potential, i.e. the difference of the Eqs. (32) and (33).

The deviation of the extended relation $\tilde{i}_{ext}$ from the numerical computations (see Fig. 5) is mainly due to the initial dip in the non-linearized Nernst equation (analogous to Fig. 3 in Ref. [1]).

Finally, the influence of the initial dip on the cell voltage is expressed by an additional term C/u_1, where C is the surface between the initial dip and the linear approximation for the equilibrium potential. The extended expression of the cell voltage as a function of the total fuel utilization u_1 is obtained from Eq. (35), analogously to the derivation of Eq. (22) in Ref. [1]

$$\tilde{V}_{cell}^{ext} \approx \tilde{V}_{eq}^{*}[0, T(0)] - \frac{1}{2}\tilde{\alpha}u_1 - \left(1 + \frac{1}{3}\tilde{Z}^2\right) r_m i_{out} + C\frac{1}{u_1} \quad (0.2 \lesssim u_1 \lesssim 0.8) \tag{41}$$

Note that C represents the same quantity as in the isothermal model, since it is not attended by a '$\sim$'. Actually, the value of C is slightly influenced by local temperature gradients. However, this dependence is so small that it has been neglected. The correction term C/u_1 is especially significant for values of u_1 between 0.2 and 0.6.

Eq. (41) is a very accurate approximation for the cell voltage in BVP(2) with non-linearized Nernst equation. In fact, the approximation for the local current density in Eq. (40) is based on the linearized Nernst equation. Nevertheless, also this latter expression was shown to be an accurate approximate solution for the non-linearized problem, for reasonably high values of u_1 up to about 0.8.

4. Conclusions

The following conclusions have been drawn from the present study:

1. A non-isothermal model for fuel cells with co-flow was developed, based on the assumptions 1 to 9 shown in the Tables 1 and 2. In this article the attention was focused on a simplified version of this model, that is also based on the additional assumptions 10 and 11 in Table 2. If these additional assumptions are also satisfied, the local temperature inside the cell depends linearly on the local fuel utilization.

2. The linear relation for the temperature simplifies considerably the non-isothermal fuel cell modeling. It is used to determine the analogous of the parameter α that describes the Nernst loss in the isothermal model. The linear relation is also suitable to express the amount of oxidant required for cooling as a function of the cell voltage, the cell current and the total increase in the cell temperature. The accuracy of this latter expression was demonstrated for an MCFC, using results of extended numerical computations. At a total fuel utilization of 95%, the deviation in the analytically calculated value for the oxidant mass supply was shown to be in the order of 0.3% only.

3. A quasi-isothermal approach was introduced. This approach provides the possibility to generalize the results and conclusions drawn from the isothermal model [1], to non-isothermal fuel cells. A quasi-isothermal parameter setting was introduced that can be used in the isothermal model, in order to determine analytical relations for non-isothermal fuel cells.

4. Analytical expressions for the local current density and the cell voltage, derived with the use of the quasi-isothermal approach, were verified to be very accurate up to high fuel utilizations, by comparison with numerical calculations.

5. A close upper bound for the cell voltage of a non-isothermal fuel cell was derived and it was shown that this upper bound is achieved if and only if the quasi-ohmic losses are homogeneously distributed over the cell (Appendix B). A homogeneous or almost homogeneous distribution of the quasi-ohmic losses is therefore favourable with respect to the cell voltage and fuel cell efficiency.

5. List of symbols

$c_{p,a}$	specific heat at constant pressure of the anode gas mixture	J/kg
$c_{p,c}$	specific heat at constant pressure of the cathode gas mixture	J/kg
C	surface between the initial dip in $V_{eq}(u)$ and the linearized function $V_{eq}^{*}(u)$	V
$E(T)$	reference potential	V
$\Delta \dot{H}$	enthalpy change per unit time	W
$\Delta \dot{H}_{thermal}$	enthalpy increase, per unit time, due to temperature rise	W
$\Delta \dot{H}_{isothermal}$	reaction heat at constant pressure per unit time	W
F	constant of Faraday	C/mol
i	local current density	A/m^2
I_{in}	total current equivalent of the fuel supply	A
i_{in}	total current equivalent of the fuel supply per unit cell surface	A/m^2
I_{out}	total current output of a fuel cell	A
i_{out}	total current output of a fuel cell per unit cell surface; average current density	A/m^2
K	equilibrium constant for concentrations in the reverse shift reaction	
$\dot{m}_a$	anode mass flow	kg/s
$\dot{m}_c$	cathode mass flow	kg/s
$\dot{Q}$	transfer of heat to a system per unit time	W
r	uniform quasi-ohmic resistance in the isothermal model	Ω m^2
$\tilde{r}$	non-uniform quasi-ohmicresistance in the non-isothermal model	Ω m^2
$\langle \tilde{r} \rangle$	average value of the quasi-ohmic resistance $\tilde{r}$	Ω m^2
r_m	a mean value of the quasi-ohmic resistance $\tilde{r}$ (see Eq. (34))	Ω m^2
R	universal gas constant	J/mol K
T	local temperature for the gas flows	K

ΔT	total temperature difference in a fuel cell (inlet to outlet)	K
$u(x)$	fuel utilization in the isothermal model	
$\tilde{u}(x)$	fuel utilization in the non-isothermal model	
$u(\tilde{u})$	invertable mapping that results in a quasi-isothermal problem formulation	
u_1	total fueli utilization	
$V_{eq}(u)$	Nernst potential in the isothermal model	V
$\tilde{V}_{eq}[\tilde{u},T]$	Nernst potential in the non-isothermal model	V
$V_{eq}^*(u)$	linear fit for $V_{eq}(u)$	V
$\tilde{V}_{eq}^*[\tilde{u},T(\tilde{u})]$	linear fit for $\tilde{V}_{eq}[\tilde{u},T(\tilde{u})]$	V
$\tilde{V}_{cell}$	cell voltage in the non-isothermal model with non-linearized Nernst equation	V
$\tilde{V}_{cell}^*$	cell voltage in the non-isothermal model with linearized Nernst equation	V
W	delivered power	W
x	scaled, i.e. relative, distance to the cell inlet	
$\tilde{Z}$	dimensionless number	

Greek letters

α	characteristic value for the derivative of $-V_{eq}(u)$ with respect to u	V
$\tilde{\alpha}$	analogous of α, for use in the non-isothermal model	V
γ	constant related to λ (see Eq. (25))	
λ	constant determined by $\tilde{r}(0)$ and $\tilde{r}(u_1)$ (see Eq. (19))	
	actiivation energy for the conduction	J/mol
χ	constant of proportion in the simplified expression for the reaction heat	V

Abbreviations

MCFC	molten carbonate fuel cell
BVP	boundary value problem
ODE	ordinary differential equation

Symbols

~	refers to the non-isothermal model
*	attends potentials that are based on a linearized Nernst equation
ext	extended relation

Acknowledgements

NEDO (Japan) is acknowledged for partly supporting this work within an International Joint Research Project. with Tohoku University (Sendai), Yokohama National University, IIT (Chicago), KTH (Stockholm) and TU Delft. The authors also wish to acknowledge A. de Groot, from TU Delft, who has provided helpful discussions. We also thank him for the use of his extended numerical cell mode (on which Fig. 3 is based).

Appendix A

A.1. The parameters $\tilde{\alpha}$, χ, r_m and i_{in}^{ext}

A.1.1. The parameter $\tilde{\alpha}$, based on the linear relation for T

In the non-isothermal model, the parameter $-\tilde{\alpha}$ represents a characteristic value for the total derivative of the equilibrium potential

$$\tilde{\alpha} = \text{constant} \approx -\left(\frac{\partial \tilde{V}_{eq}}{\partial \tilde{u}}[\tilde{u},T(\tilde{u})]\right)_T - \frac{dT}{d\tilde{u}}\frac{\partial \tilde{V}_{eq}}{\partial T}[\tilde{u},T(\tilde{u})] \text{ for most } u \in (0,1) \quad \text{(A1)}$$

where the index T indicates that the derivative holds for a fixed temperature. This derivative is equal to the parameter α in the isothermal model by definition. Furthermore, the derivative of T with respect to $\tilde{u}$ easily follows from the linear relation

for the local temperature derived in Section 2 (Eq. (13)). For instance, for the MCFC considered in Section 3, based on Eq. (15), the expression for $\tilde{\alpha}$ can be rewritten as

$$\tilde{\alpha} \approx \alpha - \frac{100}{u_1}\frac{\partial \tilde{V}_{eq}}{\partial T}[\tilde{u},T(\tilde{u})] \tag{A2}$$

The partial derivative of the equilibrium potential with respect to T is determined from Eq. (20) (recall that K was considered to be independent of T, in this equation). Also using the linear approximation for the equilibrium potential in the isothermal model, at an average temperature of 923 K, we successively obtain

$$\frac{\partial \tilde{V}_{eq}}{\partial T}[\tilde{u},T(\tilde{u})] = \frac{\partial E}{\partial T} - \frac{R}{2F}f(\tilde{u}.K) \approx \frac{\partial E}{\partial T} - \frac{\alpha \tilde{u}}{923} \tag{A3}$$

Analogously to the determination of the parameter α in the isothermal MCFC model [1], it is convenient to determine $\tilde{\alpha}$ in the point of inflection of the equilibrium potential. Since this point must be in the neighbourhood of $\tilde{u} = 0.5$ [1], we set $\tilde{u} = 0.5$ in Eq. (A3). The result approximates the average value of $\partial \tilde{V}_{eq}/\partial T$ over the interval [0, 1]. Substitution of this approximate value into Eq. (A2) yields a suitable characteristic value for $\tilde{\alpha}$ (see also Eq. (21) Note that a small improvement can be achieved if $f(o,s,k)$ is more closely approximated by adding the difference between V_{eq}^{*} and $V_{eq}(0)$.

So far, the temperature dependence of K was neglected. For the sake of completeness we will now investigate the inaccuracy due to this simplification. When the K in Eq. (44) is considered as a function of temperature, this equation can still be elaborated as previously explained. The chain rule for differentiation then yields

$$\frac{\partial \tilde{V}_{eq}}{\partial T}[\tilde{u},T(\tilde{u})] \approx \frac{\partial E}{\partial T} - \frac{\alpha \tilde{u}}{923} - \frac{dK}{dT}\frac{\partial \alpha}{\partial K}\tilde{u} \tag{A4}$$

A typical value for the derivative $(dK/dT)(\partial\alpha/\partial K)$ is obtained from the linear approximation $[\alpha(K = 0.67) - \alpha(K = 0.4)]/100$, where $\alpha(K)$ follows from the isothermal model at 650 °C by using adapted values for K, corresponding with 700 or 600 °C, respectively. For the standard fuel composition (Table 3), the derivative is typically $10^{-4} \times V/K$ and the last term in Eq. (A4) contributes about 6 mV to the value of $\tilde{\alpha}$ ($u_1 = 0.8$).

Nevertheless, for the standard fuel composition, the actual difference in the calculated values for $\tilde{\alpha}$ appears to be considerably less than 6 mV. Because, in fact, E depends on $K(T)$ and so the values for $\partial E/\partial T$ in Eqs. (A3) and (A4) are different. Consequently, for the standard fuel composition, these equations generate almost the same value for $\partial \tilde{V}_{eq}/\partial T$.

A.1.2. The parameter χ, for the cell reaction $H_2 + 1/2O_2 \rightarrow H_2O$

If the enthalpy of formation $\Delta h_{isot}^{H_2O}$ of 1 mole of water is known, the corresponding value of χ can easily be calculated. For instance, at 600 °C and atmospheric pressure, $\Delta h_{isot}^{H_2O}$ is equal to -247 kJ/mol (based on the JANAF tables). The electrical current, corresponding with the electrochemical conversion of hydrogen is given by Faraday's law, being $2F$ A/mol hydrogen. The parameter $-\chi$ was defined in Section 2.2.2, as the ratio of the reaction heat and the cell current. Hence, for the reaction of hydrogen with oxygen, χ is given by

$$\chi = -\frac{\Delta h_{isot}^{H_2O}}{2F} = 1.28\text{V}$$

If also the shift reaction occurs, it is convenient to use a slightly adapted value for χ. Below, a suitable correction term will be introduced that depends on the inlet fuel composition and the total fuel utilization u_1. The mole fractions of H_2 and CO at the anode inlet, at equilibrium, are respectively denoted by $X_1(0)$ and $X_2(0)$. Furthermore, Δh_{isot}^{shift} refers to the reaction heat of the shift reaction (-36 kJ/mol at 600 °C and atmospheric pressure). In order to calculate the amount of CO converted by the shift reaction we consider two alternative subprocesses. In the first subprocess, the inlet fuel composition is heated to the outlet temperature of the fuel cell and the gas composition changes only as a result of variations in $K(T)$. The amount of moles of CO converted in this first step is given by $X_2(0;K_{inlet}) - X_2(0;K_{outlet})$ times the total (and constant) number of moles in the fuel flow. The constants K_{inlet} and K_{outlet} represent the equilibrium constant for the reverse shift reaction at the inlet and outlet temperature, respectively. In the second step, the fuel is converted by an isothermal fuel cell. The amount of CO converted in this latter step is proportional to $X_2(0;K_{outlet}) \times v(u_1;K_{outlet})$ (the explicit expression for the reaction coordinate $v(u_1)$ is given in Ref. [1]). The modified value of χ represents the ratio of the total reaction heat and the cell current

$$\chi = -\frac{\Delta h_{isot}^{H_2O}}{2F} - \left\{\frac{X_2(0;K_{inlet}) - X_2(0;K_{outlet})[1 - v(u_1;K_{outlet})]}{[X_1(0) + X_2(0)]u_1}\right\}\frac{\Delta h_{isot}^{shift}}{2F}$$

A.1.3. The parameter r_m

In fact, the mean value r_m for the quasi-ohmic resistance is the limiting value of the following combined iteration process

$$\begin{cases} \dfrac{du_i}{dx} = \dfrac{1}{i_{in} r_i}\left(\tilde{V}^*_{eq}[0;T(0)] - \tilde{\alpha} u_{i-1} - \tilde{V}^*_{cell}\right), \quad u_i(0) = 0, \quad i = 3,4,5,\ldots \\ r_{i+1} = \dfrac{r_i}{u_1}\displaystyle\int_0^{u_1} \frac{\tilde{V}^*_{eq}[0;T(0)] - \tilde{\alpha} u_i - \tilde{V}^*_{cell}}{\tilde{V}^*_{eq}[0;T(0)] - \tilde{\alpha} u_{i-1}(u_i) - \tilde{V}^*_{cell}} du_i, \quad i = 3,4,5,\ldots \end{cases}$$

with the following initial values, defined in Section 3

$$u_2(x) = \tilde{u}(x) \quad (0 \le x \le 1) \quad r_3 = \langle \tilde{r} \rangle$$

Recall that the constant u_1 is used to denote the total fuel utilization. The derivation of the ODE for $i = 3$ has been explained in Section 3, omitting the index '3'. It was shown how the variable quasi-ohmic resistance in the ODE for $\tilde{u}$ is replaced by its average value $r_3 \equiv \langle \tilde{r} \rangle$. Attention was also paid to the linearization of the ODE for $i = 3$ and the corresponding artificial loss in equilibrium potential. All next iterations are based on the same principle. However, now an exact correction for the artificial loss in equilibrium potential is made, by a local adaption of the average quasi-ohmic resistance, instead of a global adaption. This yields a 'quasi-ohmic resistance' that depends on position again, which give rise to the next iteration cycle: the calculation of the average value r_4 and the function u_4.

Theoretically this process can be continued, and the quantities $u_3(x)$, r_4, $u_4(x)$, r_5,... can successively be obtained from the iteration process. For the same reason as given in Section 3 for the first step, the end condition $u_i(1) = u_1$ will hold for all i. Consequently, all r_i must lie within limits that are independent of i. Because otherwise the end condition cannot be satisfied for some i, since the derivative du_i/dx in the corresponding ODE would be too large (or too small). Furthermore, it can be shown that $u_i(x) \ge u_{i-1}(x)$ for all i, and that r_i is monotone decreasing with respect to i [8]. So, r_i converges to a limit r_m as i tends to infinity. This implies that u_i converges to a limiting function, which satisfy BVP(1') in Section 3. This limiting function will be denoted by u_∞. In Section 3.3, an accurate approximation for r_m was used, which will be derived below. The expression for the cell voltage derived in Section 3.3 is accurate. But the difference between $u_3(x)$, referred to as $u(x)$, and $u_\infty(x)$ was neglected. Consequently, the expression for the local current density, derived in Section 3.3, is somewhat less accurate, since it is, in fact, based on the function u_∞ instead of the required u.

Assuming that the maximum difference between $u_3(x)$ and $u_\infty(x)$ is small, an accurate analytical approximation for r_m can be derived as follows. Dividing the ODEs for $u_\infty(x)$ and $u_3(x)$ we obtain (also using the initial settings for u_2 and r_3)

$$\frac{du_\infty}{du_3} = \frac{\langle \tilde{r} \rangle}{r_m} \frac{\tilde{V}^*_{eq}[0;T(0)] - \tilde{\alpha} u_\infty - \tilde{V}^*_{cell}}{\tilde{V}^*_{eq}[0;T(0)] - \tilde{\alpha} \tilde{u} - \tilde{V}^*_{cell}}$$

By setting $u_\infty(x) = u_3(x)$ on the right-hand side of this equation (recalling that $u_\infty(x) \ge u_3(x)$) and integrating the result from $u_3 = 0$ to $u_3 = u_1$, we obtain

$$r_m \le \frac{\langle \tilde{r} \rangle}{u_1} \int_0^{u_1} \frac{\tilde{V}^*_{eq}[0;T(0)] - \tilde{\alpha} u_3 - \tilde{V}^*_{cell}}{\tilde{V}^*_{eq}[0;T(0)] - \tilde{\alpha} \tilde{u}(u_3) - \tilde{V}^*_{cell}} du_3 \tag{A5}$$

where also the end condition $u_\infty(1) = u_1$ is used. Next, from a suitable standard expansion of the right-hand side of this equation, it can be shown that the following upper bound is fairly close to the exact value of r_m

$$r_m \le \langle \tilde{r} \rangle \left(1 - \frac{a}{u_1} \int_0^{u_1} [u - \tilde{u}(u)] du\right) \tag{A6}$$

with

$$a = \frac{\tilde{\alpha}}{\tilde{V}^*_{eq}[0;T(0)] - \tilde{V}^*_{cell}} \approx \frac{2\tilde{\alpha}}{(\tilde{\alpha} + 2\langle \tilde{r} \rangle i_{in}) u_1}$$

The approximation for a is based on the so-called double linear relation or zero order approximation for the cell voltage, obtained by omitting the last term in Eq. (35) (see Ref. [1]; without a further loss in accuracy r_m is replaced by $\langle \tilde{r} \rangle$ in the approximation for a).

[8] Under the condition that $\tilde{r}(\tilde{u})$ is a monotone decreasing function of $\tilde{u}$. In the general case, the inequality $u_i \ge u_{i-1}$ is not necessarily valid and the proof of convergence is somewhat more extended.

In specific cases, the expression for r_m given in Eq. (A6) (or a more complete expansion of Eq. (A5)) can be elaborated by using the inverse mapping $\tilde{u}(u)$. The expression for r_m that was given in Section 3.3 (Eq. (34)), is obtained by using the mapping in Eq. (31).

A.1.4. The parameter i_{in}^{ext}

The extended expression for the local current density given in Section 3.4 is obtained from a linearization around the limiting solution u_∞. This linearization makes it possible to bypass the iterations for $i \geq 4$ in a more accurate way than by neglecting the difference between u_3 and u_∞. Here, the main point of this exercise will be highlighted, i.e. the introduction of the parameter i_{in}^{ext}.

The limiting solution u_∞ is based on the parameter value r_m, whereas the function u_3 is based on the parameter value $\langle \tilde{r} \rangle$. However, both functions correspond with the same cell voltage, since this quantity remains unchanged by the iteration process. Hence, both functions must also correspond with the same 'total resistance' that determines the cell voltage. In the isothermal model (see Eq. (25) in Ref. [1]) it was shown that this total resistance consist of the load resistance, the uniform quasi-ohmic resistance and the 'utilization resistance', being equal to $\alpha/2i_{in}$. The utilization resistance depends on the equivalent input current density i_{in}. When switching from a quasi-ohmic resistance $\langle \tilde{r} \rangle$ to a quasi-ohmic resistance r_m (i.e. bypassing the iterations for $i \geq 4$) the equivalent input current density has to be adapted in such a way, that the total resistance remains constant. Of course this is a mathematical trick and does not affect the real value of i_{in}. So, the parameter i_{in}^{ext} easily follows from the required change in the utilization resistance, determined by

$$\frac{\tilde{\alpha}}{2i_{in}} + \langle \tilde{r} \rangle = \frac{\tilde{\alpha}}{2i_{in}^{ext}} + r_m \tag{A7}$$

It can be made clear that this equation for i_{in}ext has to be be used in combination with Eq. (A6) for r_m. Recall from Eq. (34), that the parameter r_m is equal to the average resistance $\langle \tilde{r} \rangle$ times the factor $(1 - \delta)$. When rewriting Eq. (48), one may approximate $\delta/(1 - \delta)$ by δ in order to obtain Eq. (39).

Eq. (A6) gives an approximation for r_m, hence for δ. The obtained expression for i_{in}^{ext} is recommended if this approximation for δ is used. However, if δ is more accurately determined, it is recommendable to use the identity $i_{in}^{ext} = i_{in}/\sqrt{1 - \delta}$ instead of Eq. (39). It can be shown that this latter identity yields the most accurate result, as long as δ is very accurately known.

Appendix B

B.1. A close upper bound for the cell voltage in BVP(2)

Denoting the average value of the square root of the quasi-ohmic resistance by $\langle \sqrt{\tilde{r}} \rangle$ (analogous to Eq. (24)), it will be shown that

$$\tilde{V}_{cell} \leq \frac{1}{u_1} \int_0^{u_1} \tilde{V}_{eq}[\tilde{u}, T(\tilde{u})] \mathrm{d}\tilde{u} - \langle \sqrt{\tilde{r}} \rangle^2 i_{out} \tag{A8}$$

with equality if and only if $\tilde{r}(x)\tilde{i}^2(x) =$ constant for all x. The upper bound in Eq. (A8) is the generalization of the upper bound for the cell voltage that was derived from the isothermal model, hence for the special case in which $\tilde{r}(x) = r$ for all x [1].

In order to show the validity of Eq. (A8) we multiply both sides of the ODE in BVP(2) by $\mathrm{d}\tilde{u}/\mathrm{d}x$ and integrate with respect to x from zero to unity. Rewriting the result, using Eq. (4), we obtain

$$\tilde{V}_{cell} = \frac{1}{u_1} \int_0^{u_1} \tilde{V}_{eq}[\tilde{u}, T(\tilde{u})] \mathrm{d}u - \frac{1}{i_{out}} \int_0^1 \tilde{r}(x)\, \tilde{i}^2(x) \mathrm{d}x \tag{A9}$$

The upper bound in Eq. (A8) is obtained by estimating the last integral in Eq. (A9).

This estimation is based on the Lemma of Cauchy–Schwarz [18,19], which states that the following inequality holds for two continuous functions $f(\tilde{u})$ and $g(\tilde{u})$

$$\left(\int_0^{u_1} f(\tilde{u})\, g(\tilde{u}) \mathrm{d}u \right)^2 \leq \int_0^{u_1} f^2(\tilde{u}) \mathrm{d}\tilde{u} \int_0^{u_1} g^2(\tilde{u}) \mathrm{d}\tilde{u} \tag{A10}$$

Applying the Lemma of Cauchy–Schwarz on the following integral

$$\langle\sqrt{\tilde{r}}\rangle \equiv \frac{1}{u_1}\int_0^{u_1}\sqrt{\tilde{r}(\tilde{u})}\cdot\frac{\sqrt{\tilde{i}(\tilde{u})}}{\sqrt{\tilde{i}(\tilde{u})}}\mathrm{d}\tilde{u}$$

by setting $f(\tilde{u})=\sqrt{\tilde{r}(\tilde{u})}\sqrt{\tilde{i}(\tilde{u})}$ and $g(\tilde{u})=1/\sqrt{\tilde{i}(\tilde{u})}$, we obtain

$$\langle\sqrt{\tilde{r}}\rangle^2 \le \frac{1}{u_1^2}\left(\int_0^{u_1}\tilde{r}(\tilde{u})\tilde{i}(\tilde{u})\mathrm{d}\tilde{u}\int_0^{u_1}\frac{1}{\tilde{i}(\tilde{u})}\mathrm{d}\tilde{u}\right) \tag{A11}$$

Using the identity $\tilde{i}(x)=i_{in}\mathrm{d}\tilde{u}/\mathrm{d}x$ (Eq. (4)), this inequality can be rewritten as

$$\langle\sqrt{\tilde{r}}\rangle^2 \le \frac{1}{i_{\mathrm{out}}^2}\int_0^1\tilde{r}(x)\tilde{i}^2(x)\mathrm{d}x \tag{A12}$$

Substitution of this inequality into Eq. (A9) yields Eq. (A8).

The Lemma of Cauchy–Schwarz also states [19], that the equality in Eq. (A10) holds if and only if $f=\text{constant}\times g$. Hence, the equality in Eq. (A11) holds if and only if $\sqrt{\tilde{r}}\sqrt{\tilde{i}}=\text{constant}/\sqrt{\tilde{i}}$. So, the cell voltage is maximum if the quasi-ohmic losses are homogeneously distributed over the cell

$$\tilde{r}(x)\tilde{i}^2(x)=\text{constant for all } x \Leftrightarrow \text{the upper bound for } \tilde{V}_{cell} \text{ in Eq. (A8) holds}$$

For the MCFC considered in Section 3 and a total fuel utilization of 80%, the deviation of the cell voltage from the obtained upper bound is 10 mV (from Eq. (41)).

Acknowledgements

NEDO (Japan) is acknowledged for partly supporting this work within an International Joint Research Project, with Tohoku University (Sendai), Yokohama National University, IIT (Chicago), KTH (Stockholm) and TU Delft.

The authors also wish to acknowledge A. de Groot, from TU Delft, who has provided helpful discussions. We also thank him for the use of his extended numerical cell model (on which Fig. 3 is based).

References

[1] F. Standaert, K. Hemmes, N. Woudstra, Analytical fuel cell modeling, J. Power Sources 63 (1996) 221–234.
[2] J.H. Hirschenhofer, D.B. Stauffer and R.R. Engleman, *Fuel Cells, A Handbook*, US Department of Energy, 1994, Ch. 2.
[3] G.H.J. Broers, High temperature galvanic fuel cells, *Ph.D. Thesis*, Amsterdam University, The Netherlands, Ch. 1, 1958.
[4] R. Courant and D. Hilbert, *Methods of Mathematical Physics. Vol. 2*, Wiley-Interscience, New York, 1962.
[5] L.A. Pipes, L.R. Harvill, *Applied Mathematics for Engineers and Physicists*, McGraw-Hill, Kogakusha, Tokyo, 3rd. edn.
[6] A. de Groot, Exergy analysis of high temperature fuel cell systems, *Ph.D. Thesis*, Delft University of Technology, The Netherlands, 1998.
[7] W.M.A. Klerks, G.J. Kraaij, G. Rietveld, MCFC stack development at ECN, *Ext. Abstr., Fuel Cell Seminar 1994, San Diego, CA, USA, 1994*, pp. 160–163.
[8] T. Watanabe, T. Abe, Y. Izaki, Y. Mugikura, E. Koda, 100 KW Class MCFC stack performance. *Ext. Abstr., Fuel Cell Seminar 1994, San Diego, CA, USA*, pp. 446–449.
[9] T. Kakihara, T. Morita, A. Suzuki, Y. Yamamasu, Development of a 100 KW MCFC stack and its components, *Ext. Abstr. Fuel Cell Seminar 1994, San Diego, CA, USA*, pp. 450–453.
[10] J.R. Selman, *Performance Models for Molten Carbonate Fuel Cells*, Molten Salt Committee of the Electrochemical Society of Japan, Feb. 1988.
[11] T. Watanabe, Y. Mugikura, Y. Izaki, E. Koda, H. Kinoshita, T. Abe, Modeling analysis on molten carbonate fuel cells and stacks, *Proc. Intersociety Energy Conversion Engineering Conf., San Diego, CA, USA, 1992*, Vol. 3, pp. 3269–3276.
[12] E. Achenbach, *J. Power Sources, 49* (1994) 333–348.
[13] G. Cao, F. Yoshiba, E. Kouda and T. Watanabe, Modeling and simulation of internal temperature conditions in molten carbonate fuel cell, *Proc. Int. Conf. Power Engineering, Shanghai, China, May 1995*, pp. 109–114.
[14] S. Takashima et al., Stack performance model of molten carbonate fuel cell, *Proc. Electrochemical Society Symp., 2nd Symp. MCFC Technology*, Proc. Vol. 90-16, 1990, pp. 378–394.
[15] D. Gidaspow and B.S. Baker, Heat transfer in a fuel cell battery, *AIChEJ, 11* (1965) 825–831.
[16] P.W. Atkins, *Physical Chemistry*, Oxford University Press, Oxford, 4th edn., 1990, pp. 53–55.
[17] J.M. Smith and H.C. van Ness, *Introduction to Chemical Engineering Thermodynamics*, McGraw-Hill, Singapore, 3rd edn., 1985, Ch. 2.
[18] E. Kreyszig, *Introductory Functional Analysis with Applications*, Wiley, New York, 1978.
[19] N. Young, *An Introduction to Hilbert Space*, Cambridge University Press, Cambridge, 1992.